

The Capabilities of the upgraded MIPP experiment with respect to HyperNuclear Physics

Rajendran Raja

For the MIPP collaboration

Fermilab, P.O. Box 500, Batavia, Illinois 60510

E-mail: raja@fnal.gov

Abstract. We describe the state of analysis of the MIPP experiment, its plans to upgrade the experiment and the impact such an upgraded experiment will have on hypernuclear physics.

1. Introduction

The upgraded MIPP experiment is designed to measure the properties of strong interaction spectra from beams π^\pm , K^\pm and p^\pm for momenta ranging from 1 GeV/c to 120 GeV/c. The layout of the apparatus in the data taken so far can be seen in Figure 1. The centerpiece of the experiment is the time projection chamber, which is followed by the time of flight counter, a multi-cell Cerenkov detector and the RICH detector. The TPC can identify charged particles with momenta less than 1 GeV/c using dE/dx , the time of flight will identify particles below approximately 2 GeV/c, the multi-cell Cerenkov detector is operational from 2.5 GeV/c to 14 GeV/c and the RICH detector can identify particles up to 120 GeV/c. Following this is an EM and hadronic calorimeter capable of detecting forward going neutrons and photons.

The experiment has been busy analyzing its data taken on various nuclei and beam conditions. The table 2 shows the data taken by MIPP I to date.

We have almost complete acceptance in the forward hemisphere in the lab using the TPC. The reconstruction capabilities of the TPC can be seen in Figure 3.

The particle identification capabilities of the TPC can be seen in Figure 4.

The time of flight system provides further measurement of the particles with momenta less than 2 GeV/c. Figure 5 shows the time of flight data where a kaon peak is clearly visible.

2. Results from data taken so far

MIPP has published forward going neutron spectra off various nuclei and compared it with Monte Carlo predictions [1]

It can be seen clearly that the Monte Carlo predictions differ significantly from each other and the data.

Figure 7 shows (in a paper in preparation, [2]) preliminary results of particle production from the full NuMI target as a function of momenta.

MIPP

Main Injector Particle Production Experiment (FNAL-E907)

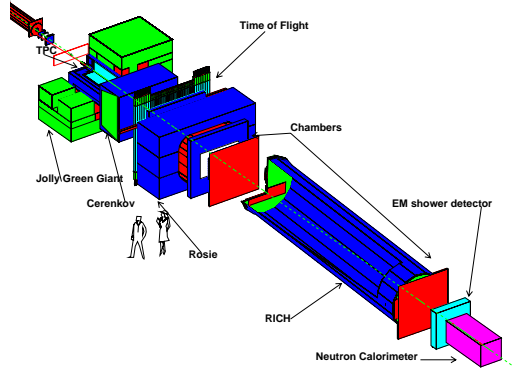


Figure 1. Layout of the experiment - Run I. With the MIPP upgrade we propose to add the plastic ball detector as a recoil detector surrounding the target.

| Data Summary 27 February 2006 | | | Acquired Data by Target and Beam Energy Number of events, $\times 10^6$ | | | | | | | | | |
|----------------------------------|----------|-------------|--|------|------|------|------|-------|------|------|------|-------|
| Target | | | E | | | | | | | | | Total |
| Z | Element | Trigger Mix | 5 | 20 | 35 | 40 | 55 | 60 | 65 | 85 | 120 | |
| 0 | Empty | Normal | | 0.10 | 0.14 | | | 0.52 | | | 0.25 | 1.01 |
| | K Mass | No Int. | | | | 5.48 | 0.50 | 7.39 | 0.96 | | | 14.33 |
| | Empty LH | Normal | | 0.30 | | | | 0.61 | | 0.31 | | 7.08 |
| 1 | LH | Normal | 0.21 | 1.94 | | | | 1.98 | | 1.73 | | |
| 4 | Be | p only | | | | | | | | | 1.08 | 1.75 |
| | | Normal | | | 0.10 | | | 0.56 | | | | |
| 6 | C | Mixed | | | | | | 0.21 | | | | 1.33 |
| | C 2% | Mixed | | 0.39 | | | | 0.26 | | | 0.47 | |
| | NuMI | p only | | | | | | | | | 1.78 | 1.78 |
| 13 | Al | Normal | | | 0.10 | | | | | | | 0.10 |
| 83 | Bi | p only | | | | | | | | | 1.05 | 2.83 |
| | | Normal | | | 0.52 | | | 1.26 | | | | |
| 92 | U | Normal | | | | | | 1.18 | | | | 1.18 |
| Total | | | 0.21 | 2.73 | 0.86 | 5.48 | 0.50 | 13.97 | 0.96 | 2.04 | 4.63 | 31.38 |

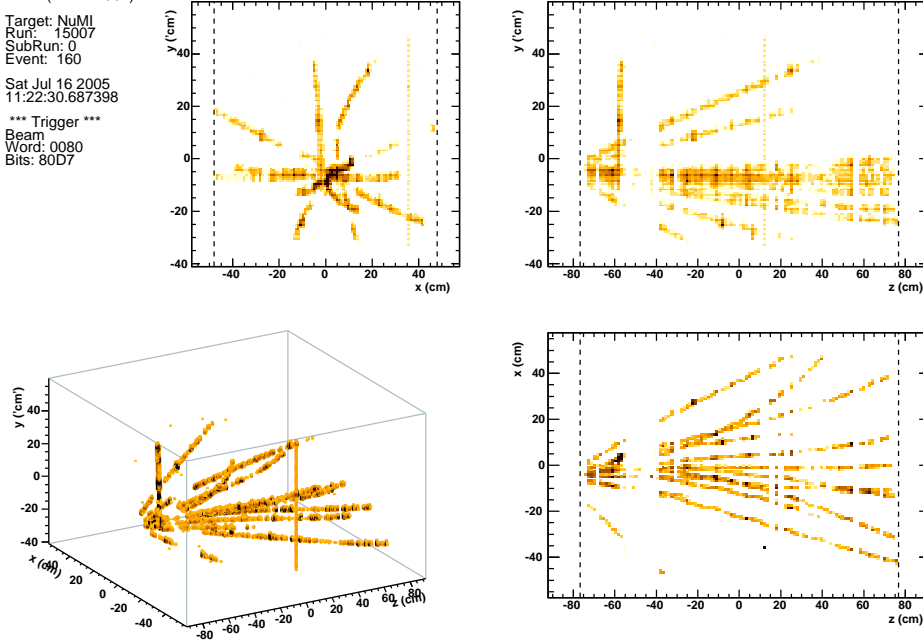
Figure 2. Data taken by MIPP I to date

3. The MIPP Upgrade proposal

The MIPP upgrade proposal consists primarily of an electronics upgrade of the whole detector so that the detector reads out at 3 kHz as compared to 20 Hz in Run I. All the new electronics modules have been prototyped. The TPC has the largest data rate and we display one of its electronics modules in Figure 8. The document [3] contains the details of the upgrade proposal. The MIPP upgrade proposal will acquire high quality data of particle production with high statistics and much improved particle identification. The available beam momenta and the calculated beam rates can be seen in table 1 and range approximately 1 GeV/c to 120 GeV/c. As such the upgrade can straddle the resonance region and the scaling region of strong interaction physics using 6 beam species. The MIPP upgrade intends to acquire data for a variety of interactions. These include

MIPP (FNAL E907)

Target: NuMI
Run: 15007
SubRun: 0
Event: 160
Sat Jul 16 2005
11:22:30.687398
*** Trigger ***
Beam
Word: 0080
Bits: 80D7



MIPP (FNAL E907)

Target: Beryllium
Run: 1219
SubRun: 0
Event: 9
Mon Feb 28 2005
03:18:40.377278
*** Trigger ***
Beam
Word: 0400
Bits: C44F

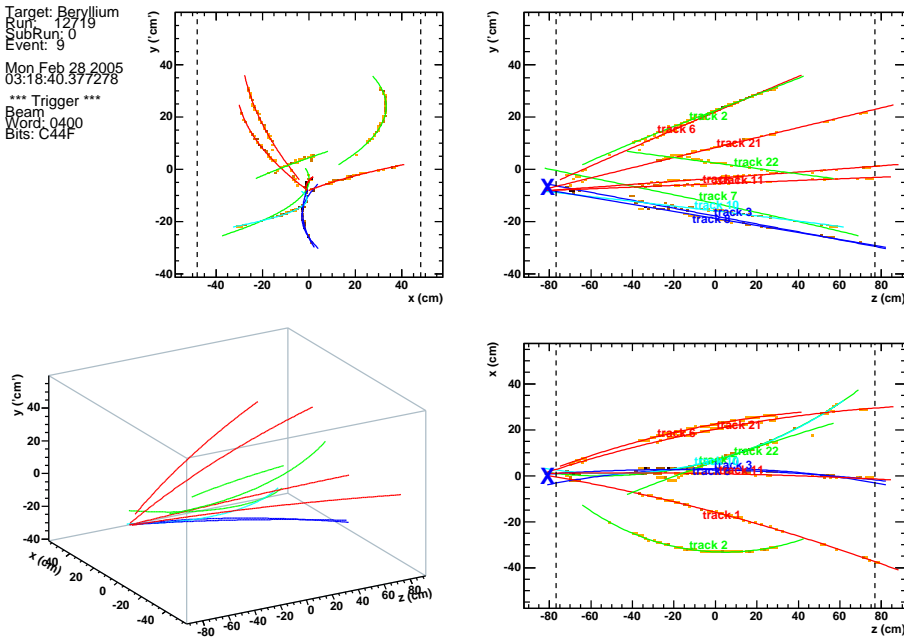


Figure 3. RAW and Reconstructed TPC tracks from two different events.

- A systematic study of missing baryon resonances between 1 GeV and 3 GeV.
- An investigation of fundamental scaling laws in inclusive reactions.
- A thorough investigation of forward neutron spectra.
- A systematic acquisition of particle production data and comparison and tuning of existing Monte Carlo generators.
- A measurement of particle production data from full scale neutrino targets and using the data to improve the target design.

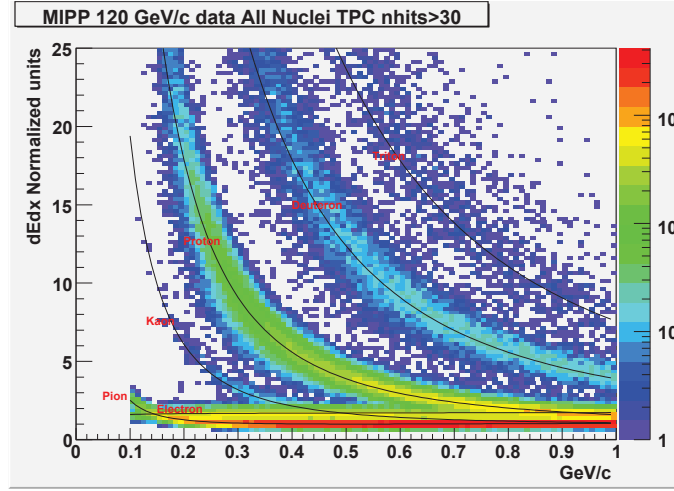


Figure 4. TPC dE/dx data from Run I. Electrons, pions, kaons and protons are distinguishable. Deuterons and tritons can also be seen

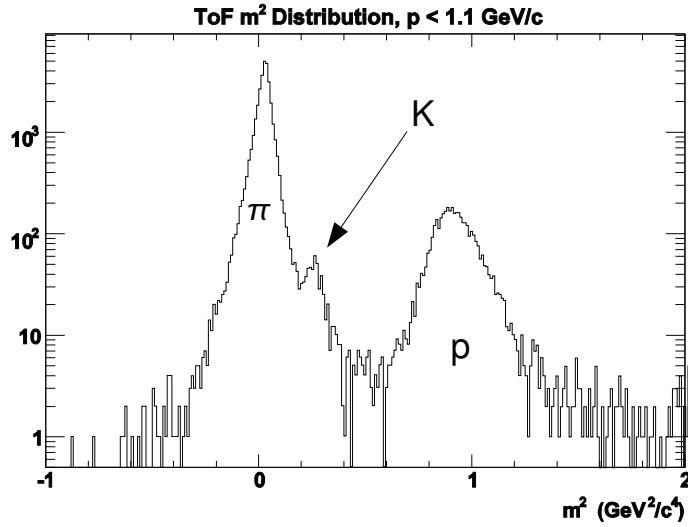


Figure 5. ToF data with momenta less than 1.1 GeV/c. a kaon peak is clearly visible.

- A systematic study of hypernuclei
- Measurement of cross section off nitrogen targets which is essential to understanding the cosmic ray showers and atmospheric neutrino production for experiments such as INO.

This is made possible since MIPP upgrade will be able to collect 5 millions events per day assuming a beam spill rate of one 4 second spill every 2 minutes,

4. Hypernuclear Physics with MIPP Upgrade

Single strange hypernuclei (with one Λ or one Σ) have production cross sections in the 100 to 250 nbarn/steradian at 1 to 2 GeV/c proton beams on nuclear targets as can be seen for Figure 9. Doubly strange hypernuclei (with two Λ) are 10 to 50 nbarn/sr with a kaon or hyperon beam on

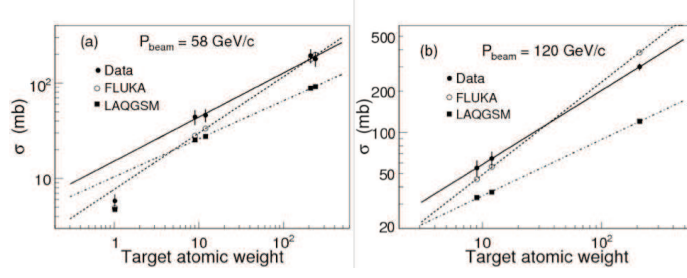


Figure 6. Comparison of the A-dependence of MIPP cross sections with those from Monte Carlos. The lines are fits to the data. The cross sections are for producing neutrons with momentum greater than the threshold and within an angular range of 20.4 mrad. The errors are combined statistical and systematic uncertainties. Note that the hydrogen data point is not included in the fit. The cross sections are not corrected for geometric acceptance.

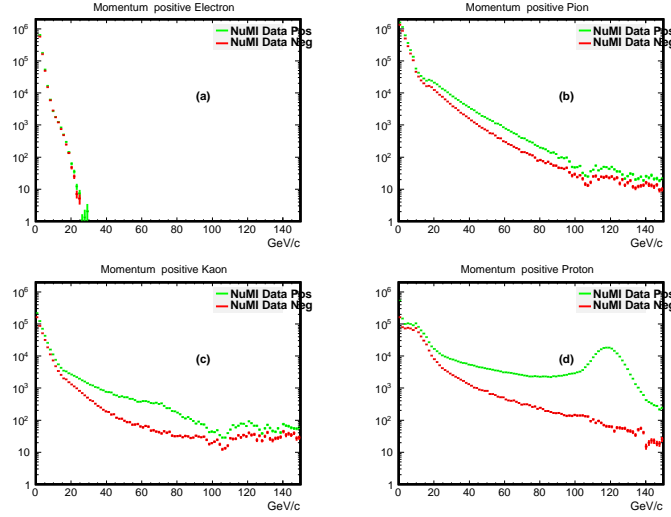


Figure 7. Analysis of NuMI target spectra (data) as a function of particle type (preliminary)

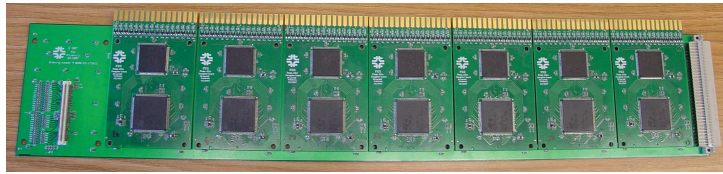


Figure 8. Electronics prototype of TPC upgrade board with ALTO/PASA chips

nuclear target and are more difficult to measure. The diagrams for doubly strange hypernuclei can be found in Figure 10. Doubly strange hypernuclei with one Ξ are not discovered yet, but 7 candidate events are known to exist. The binding energies for nuclei as a function of atomic weight can be found in Figure 11. The binding energies decrease with atomic weight indicating that the hypernuclei are less tightly bound as atomic weight increases. This behavior is also reflected in the lifetimes plot in Figure 12 where the lifetimes of the bound lambda is seen to decrease with increasing atomic weight.

Using MIPP upgrade, we have complete forward acceptance using the TPC and full particle

| momentum GeV/c | p | K ⁺ | π^+ | momentum GeV/c | \bar{p} | K ⁻ | π^- |
|-------------------|----------|----------------|----------|-------------------|-----------|----------------|---------|
| 1 | 5752 | 0 | 64798 | 1 | 7907 | 0 | 30425 |
| 2 | 23373 | 194 | 459718 | 2 | 26863 | 142 | 236494 |
| 3 | 53431 | 3060 | 1069523 | 3 | 51424 | 2221 | 598742 |
| 5 | 153220 | 32763 | 2400799 | 5 | 103996 | 23164 | 1550810 |
| 10 | 663916 | 223210 | 5006708 | 10 | 195767 | 142777 | 3862225 |
| 15 | 1618120 | 443557 | 7141481 | 15 | 221602 | 245868 | 5248463 |
| 20 | 3113387 | 655426 | 9290219 | 20 | 212171 | 306685 | 5841030 |
| 30 | 8158054 | 1043430 | 12770579 | 30 | 160329 | 340144 | 5837467 |
| 40 | 16664431 | 1294189 | 13944272 | 40 | 101617 | 288728 | 5156862 |
| 50 | 29288928 | 1338452 | 12788523 | 50 | 53056 | 196400 | 4114582 |
| 60 | 45985629 | 1191744 | 10094311 | 60 | 22092 | 108032 | 2905091 |
| 70 | 65227010 | 919279 | 6834097 | 70 | 6987 | 47093 | 1762060 |

Table 1. Calculated Beam rates for 2×10^{11} protons on primary target for MIPP upgrade

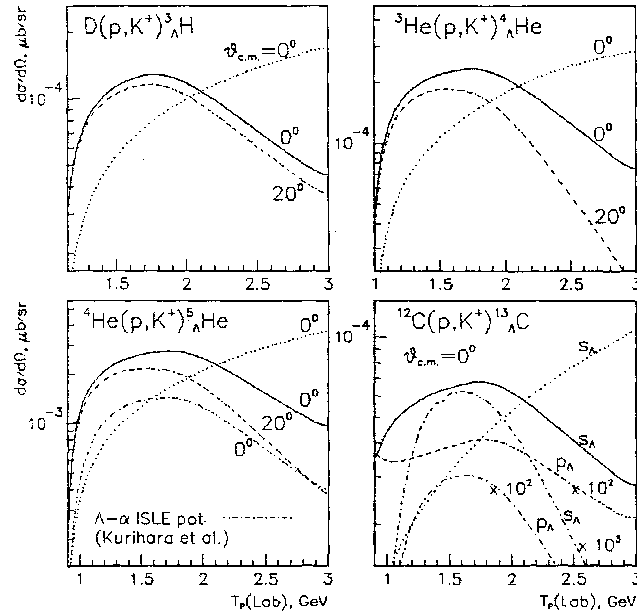


Figure 9. Differential cross sections of single hyper nucleus production on various nucleus with a proton beam and a final state kaon [4]

identification (using the TPC and the time of flight) for particles of momentum less than 1.5 GeV/c. In the backward hemisphere in the lab frame, we have the plastic ball that catches recoil particles.

We investigate the channels that are likely to yield hypernuclei. We employ the high energy physics notation to denote the reactions.

The channels involving a π^+ beam can be denoted by

$$\pi^+ + p \rightarrow \pi^+ + K^+ + \Lambda \quad (1)$$

In the above equation, π^+ beam remains a π^+ beam and fragments a proton target to form a K^+ and a Λ . Such reactions are called diffractive dissociations of the target and these maintain

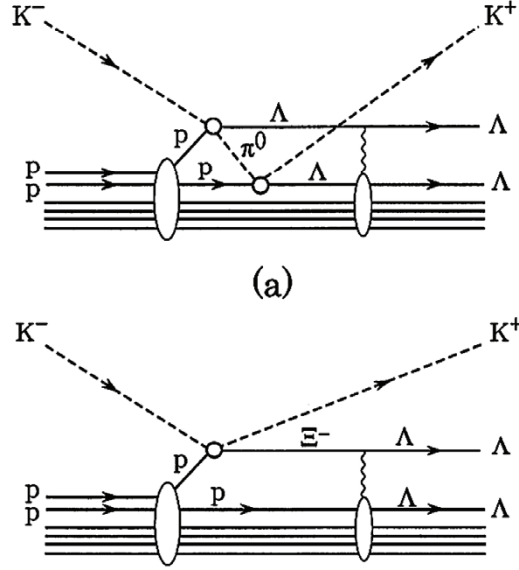


Figure 10. Mechanisms for producing double hypernuclei using a K^- beam. K^+ beams can study the background to this process [5]

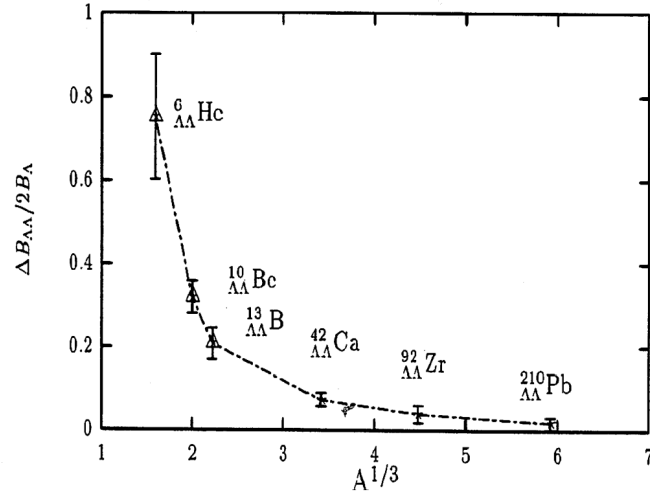


Figure 11. Binding energy of hypernuclei as a function of atomic weight.

a large cross section as the beam energy increases. The K^+ in the final state is detected by the TPC and the time of flight systems and the Λ is absorbed in the nucleus to make the hypernucleus. There may be other particles in the final state, which the particle identification of MIPP will ensure contain a net strangeness of zero. The counterpart of the above reaction with a neutron target can be written

$$\pi^+ + n \rightarrow \pi^+ + K_S^0 + \Lambda \quad (2)$$

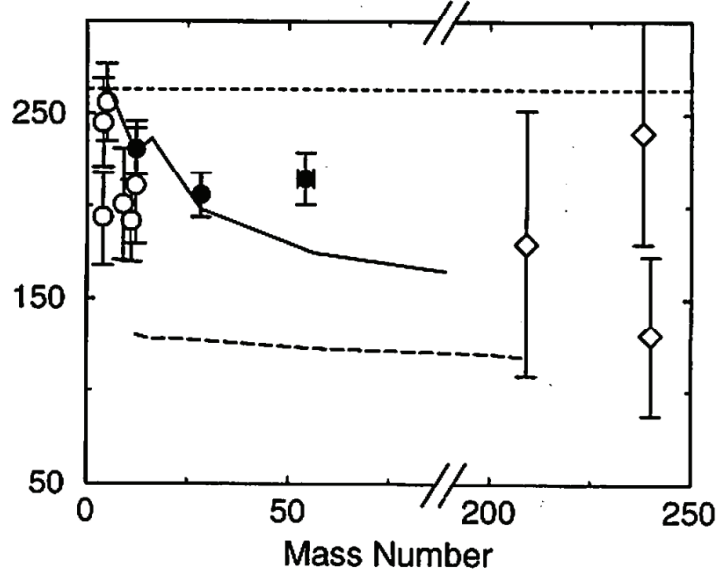


Figure 12. Lifetimes of hypernuclei as a function of atomic weight A . As A increases, lifetimes get shorter, implying less tightly bound hyper nuclei

The K_s^0 in the final state can be detected by the TPC. Similarly with a proton beam

$$p + p \rightarrow p + K^+ + \Lambda \quad (3)$$

$$p + n \rightarrow p + K_S^0 + \Lambda \quad (4)$$

These form the proton counter part. Using a K^- beam, one can look for the reaction

$$K^- + p \rightarrow \pi^+ + \Lambda \quad (5)$$

$$K^- + n \rightarrow \pi^0 + \Lambda \quad (6)$$

One can test the backgrounds to this reaction using K^+ beams which should not produce hypernuclei.

5. Conclusions

The high acceptance and particle identification of MIPP upgrade promises to produce a high quality hypernucleus experiment. This work was done at Fermilab operated by Fermi Research Alliance, LLC under Contract No. De-AC02-07CH11359 with the United States Department of Eneegy.

References

- [1] "Forward Neutron Production at the Fermilab Main Injector", T. S. Nigmanov et al Phys. Rev. D83 (2011)012002.

- [2] “Measurement of Particle Production on the NuMI target with a 102 GeV/c proton beam in the MIPP Experiment”, paper in preparation.
- [3] A copy of the MIPP upgrade proposal may be found at <https://mipp-docdb.fnal.gov:440/cgi-bin/ShowDocument?docid=104>
- [4] V. N. Fetisov, Nucl. Phys. A639 (1998), p177.
- [5] H. C. Bhang et al., Nucl. Phys. A639 (1998), p269 and 270
- [6] S. Ajimura et al., Nucl. Phys. A639 (1998) p 93-99